

Normal and hot-electron magnetophonon resonance in a GaAs heterostructure

P. Warmenbol, F. M. Peeters, and J. T. Devreese*

Department of Physics, University of Antwerp (U.I.A.), Universiteitsplein 1, B-2610 Wilrijk-Antwerpen, Belgium

(Received 20 July 1987)

Linear and nonlinear magnetophonon resonances are investigated in a two-dimensional electron gas in a single-interface GaAs-Al_xGa_{1-x}As heterostructure, within the momentum-balance equation approach. The linear transverse resistivity obtained from the present approach reduces to the high-magnetic-field result based on the Kubo formula. The Landau-level broadening is taken to be Gaussian with a constant background. We find that a Lorentzian broadening of the density of states gives slightly different results from our Gaussian broadening even when a constant background term is included. The effect of the broadening parameters on the shape of the magnetophonon oscillations in the transverse resistivity ρ_{xx} , the energy relaxation rate, and the warm-electron coefficient, is found to be appreciable and stronger than in the corresponding three-dimensional case. The nonlinear momentum-balance equation is solved for arbitrary average electron velocity. We find that the maxima at the linear magnetophonon resonance evolve to minima (and the minima become maxima), when the average electron velocity is sufficiently large.

I. INTRODUCTION

The magnetophonon resonances in the magnetoconductivity, predicted by Gurevich and Firsov,¹ occur when the LO-phonon energy matches the separation between two Landau levels: $n\hbar\omega_c = \hbar\omega_{LO}$, $n=1,2,\dots$, where ω_c is the cyclotron frequency ($\omega_c = eB/cm^*$), m^* the electron (hole) effective mass, $\hbar\omega_{LO}$ the LO-phonon energy, and B the magnetic field. The resonant character of this effect makes it a powerful spectroscopic tool. It provides useful information on phonon frequencies and band structure (i.e., the effective mass m^*). The magnetophonon effect has been investigated in detail for three-dimensional (3D) systems²⁻⁴: (i) at high temperatures ($T > 100$ K) in low electric fields (linear regime) where the LO-phonon absorption prevails (normal magnetophonon resonance effect), as well as (ii) at low temperatures in heating electric fields, where the LO-phonon emission process dominates. The review paper of Nicholas² also includes some recent experimental results on the magnetophonon resonance effect in two-dimensional (2D) systems, which have attracted theoretical interest.⁵⁻⁷

To date only a few experimental observations of the magnetophonon resonance effect have been made in 2D systems like GaAs-Al_xGa_{1-x}As and Ga_xIn_{1-x}As-InP single heterostructures and superlattices, and Ga_xIn_{1-x}As-Al_yIn_{1-y}As single heterostructures (see, e.g., Refs. 8-14). They reveal several interesting properties: (1) the conduction in these systems is 2D-like up to high temperatures (≈ 250 K), (2) magnetophonon oscillations persist up to high temperatures (≈ 250 K), (3) from the magnetophonon resonance spectra of the 2D electron gas (2D EG) in GaAs-Al_xGa_{1-x}As heterostructures,⁹ values for the LO-phonon frequency were deduced which are smaller than the values for bulk GaAs, and (4) in Ga_xIn_{1-x}As-InP superlattices¹² two series of resonances were observed, corresponding to two LO-

phonon modes and it was found that their relative intensity depends on the layer thickness. Two reports on the observation of 2D EG hot-electron magnetophonon resonance are available, both in a GaAs-type system,^{15,16} but unfortunately the data are scarce and consequently these data cannot lead to detailed comparison with the present calculations. Recently Eaves and co-workers^{17,18} studied experimentally the electric-field-induced damping of the magnetophonon resonance amplitudes in an $n^+-n^-n^+$ GaAs structure and observed a conversion of the magnetophonon resonance maxima into minima when the electric field was increased beyond the linear limit.

The aim of the present paper is to analyze the resistivity of electrons, interacting with polar LO phonons in a 2D system subjected to high magnetic fields, and to dc electric fields ranging from very small (linear regime) to large (hot-electron regime). In the study of magnetophonon resonances, the interaction with LO phonons is the dominant scattering mechanism. We will concentrate on the main trends and on a comparison of these trends with the 3D case. Numerical calculations will be performed for a 2D EG in a single-interface GaAs system. It is reasonable to assume that the electrons interact with the bulk GaAs LO-phonon mode (see Ref. 2).

Thornber and Feynman¹⁹ applied the Feynman path integral technique to study dissipative transport in electron-phonon systems in an external electric field. The rate of momentum loss and energy loss (momentum and energy balance) by an electron drifting through the crystal is written in a form in which the phonons are eliminated exactly. Peeters and Devreese²⁰ rederived the Thornber-Feynman expression for the one-oscillator model of Feynman in the framework of the Heisenberg equations of motion. In this paper the Thornber-Feynman theory is applied for the case of a nonzero magnetic field and weak electron-phonon interaction. The transition matrix elements are calculated in the first Born approximation. We will consider an effective-mass

approximation for the electrons, interacting with bulk polar LO phonons (large Fröhlich polaron). As a first approximation we take the phonons in equilibrium, although for hot-electron transport at liquid-helium temperature there exists experimental evidence^{21,22} that the phonon population may be out of equilibrium. Screening of the electron-phonon interaction will be neglected, but Fermi-Dirac statistics is retained. Unless explicitly stated, a parabolic conduction band is taken for the electrons. It is assumed that the electrons populate only the lowest electric subband, which will be described by the Fang-Howard (see, e.g., Ref. 23) variational wave function.

Application of the Thornber-Feynman theory to transport in a 2D EG in crossed electric and magnetic fields leads to an expression for the electric field as function of the average velocity of the electron system which exhibits singularities. This singular behavior is traced back to the singular nature of the unperturbed 2D electronic density of energy states, which consists of a series of δ -function peaks equally spaced by the cyclotron energy. Interaction of the 2D EG with impurities, phonons, surface roughness, and potential fluctuations in general will broaden these δ -function peaks in the density of states and, consequently, will remove the singularities in the electronic response. Recent experimental investigations²⁴⁻²⁷ of the 2D EG in both GaAs and Si structures in strong magnetic fields give evidence for a Gaussian broadening of the density of states superimposed on a flat background. There is as yet no completely satisfactory theoretical description of the 2D density of states (but see, e.g., Refs. 23, 28, and 29). Both potential fluctuations close to the interface and residual impurities in the GaAs may play a role. Gerhardt and Gudmundsson^{30,31} proposed a statistical model for spatial inhomogeneities of the electron density in a 2D EG which simulates the electrostatic potential fluctuations. The model yields an effective background density of states between Landau levels and seems to agree with the experimental observations of Refs. 24-27. Motivated by these results a *Gaussian form with a flat background* will be taken for the 2D density of states and the sensitivity of the magnetophonon resonances to the actual form of the density of states will be investigated.

The linear magnetophonon resonance effect has been studied recently by Lassnig and Zawadzki⁵ for single heterostructures and by Vasilopoulos⁶ for quantum well structures. In Refs. 5 and 6 the transverse conductivity σ_{xx} was calculated starting from the Kubo formula and in Ref. 5 a Lorentzian broadening of the density of states was introduced, while here we start from the momentum-balance equation and take a Gaussian form for the broadening. Since broadening is crucial for a quantitative analysis of the experimental data, we will stress the effect of different types of broadening.

The organization of the present paper is as follows. The resistivity obtained from the present momentum-balance-equation approach will be studied in Sec. II in the linear-response regime. Numerical results will be given for a 2D EG in a single-interface GaAs system, for which we will consider a single dispersionless LO-

phonon mode. A comparison is made with other theories and available experimental data. The emphasis will be on the dependence of the magnetophonon resonances on temperature, broadening parameters of the density of states, electron density, and width of the 2D electron layer. Hot-electron effects are studied in Sec. III within a simple electron temperature model. The effect of the heating of the 2D electron subsystem on the magnetophonon resonances and the electron energy relaxation will be investigated theoretically. Section IV gives an outline of the calculation of the nonlinear resistivity. In analogy with 3D a warm-electron coefficient is defined and studied numerically. A comparison is made with the behavior in 3D semiconductor systems and the major trends are analyzed. Our conclusions are presented in Sec. V.

II. MOMENTUM-BALANCE EQUATION

The momentum-balance equation (see Ref. 20) is given by

$$e[\mathcal{E} + (\mathbf{v} \times \mathcal{B})] = \mathbf{F}(\mathbf{v}), \quad (1)$$

where \mathcal{E} is the total electric field, \mathbf{v} is the average electron velocity, and

$$\begin{aligned} \mathbf{F}(\mathbf{v}) = & \frac{1}{N_e} \sum_{\mathbf{q}} \frac{\mathbf{q}}{\hbar} |V_{\mathbf{q}}|^2 \\ & \times \int_{-\infty}^{\infty} dt \{ [1 + n(\omega_{\mathbf{q}})] e^{it(\omega_{\mathbf{q}} - \mathbf{q} \cdot \mathbf{v})} \\ & - n(\omega_{\mathbf{q}}) e^{-it(\omega_{\mathbf{q}} - \mathbf{q} \cdot \mathbf{v})} \} S(\mathbf{q}, t) \end{aligned} \quad (2)$$

is the force exerted on the electron by the interaction with LO phonons. $S(\mathbf{q}, t) = \text{Tr}\{f(H)e^{-i\mathbf{q} \cdot \mathbf{r}(t)}[1 - f(H)]e^{-i\mathbf{q} \cdot \mathbf{r}(t)}\}$ is the space Fourier transform of the electron density-density correlation function, where the trace (Tr) is over all electron Landau states in a magnetic field and H is the electron Hamiltonian. e is the electron charge, N_e the electron density, \mathbf{v} the steady-state velocity of the electron, $\omega_{\mathbf{q}}$ the phonon frequency with phonon wave vector \mathbf{q} , and $n(\omega_{\mathbf{q}})$ is the phonon occupation number. \mathbf{r} is the electron coordinate and $f(E)$ is the Fermi-Dirac function.

Equation (2) has the same explicit form as the Thornber-Feynman result.¹⁹ The time representation of the force $\mathbf{F}(\mathbf{v})$ may be converted into a frequency representation. Making use of identities like $f(E)[1 - f(E - \hbar\omega_{\mathbf{q}})] = [f(E - \hbar\omega_{\mathbf{q}}) - f(E)]n(\omega_{\mathbf{q}})$ and Fourier-transforming the electron density-density correlation function to frequency space,^{32,33} Eq. (2) can be converted into

$$\begin{aligned} \mathbf{F}(\mathbf{v}) = & \frac{2}{N_e} \sum_{\mathbf{q}} \frac{\mathbf{q}}{\hbar} |V_{\mathbf{q}}|^2 [n(\omega_{\mathbf{q}}) - n(\omega_{\mathbf{q}} - \mathbf{q} \cdot \mathbf{v})] \\ & \times \text{Im}[D'(\mathbf{q}, \omega_{\mathbf{q}} - \mathbf{q} \cdot \mathbf{v})] \end{aligned} \quad (3a)$$

with $\text{Im}[D'(\mathbf{q}, \omega)]$, the imaginary part of the retarded density-density correlation function

$$\text{Im}[D'(q, \omega)] = -\frac{1}{2\pi^2 l^2} \sum_{n,m=0}^{\infty} J_{n,m}(\frac{1}{2} l^2 q^2) \int_{-\infty}^{\infty} dE [f(E) - f(E + \omega)] \text{Im}[G_n(E + \omega) \text{Im} G_m(E)], \quad (3b)$$

where

$$J_{n,n+j}(x) = \frac{n!}{(n+j)!} x^j e^{-x} [L_n^j(x)]^2,$$

$L_n^j(x)$ is the associate Laguerre polynomial, $\text{Im}[G_n(E)]$ is the imaginary part of the Green's function for Landau level n , and $l = (\hbar/eB)^{1/2}$ is the magnetic length.

It turns out that Eq. (3) is identical to the result of Cai, Lei, and Ting [Eq. (2) of Ref. 33], if one puts the electron temperature equal to the lattice temperature (T) and replaces \mathbf{v} by $-\mathbf{v}$ in their expression. These authors also incorporated the effect of screening and applied the balance equation approach to investigate the breakdown of dissipationless transport in the quantum Hall regime.

From the momentum-balance equation (we choose \mathbf{v} along the x axis) the resistivity components are obtained as follows:

$$\rho_{xx} = \mathbf{v} \cdot \mathbf{F}(\mathbf{v}) / [N_e (ve)^2], \quad (4a)$$

$$\rho_{xy} = \mathcal{B} / (eN_e). \quad (4b)$$

III. THE LINEAR REGIME

In this section the linear magnetoresistance of a 2D EG will be investigated. Therefore take the limit for small electron velocities, i.e., $\mathbf{v} \rightarrow 0$ in Eq. (3),

$$S(\mathbf{q}_\perp, t) = N_e \exp \left\{ -\frac{\hbar^2 q_\perp^2}{2m^* \hbar \omega_c} \{ [1 + 2n(\omega_c)] - [1 + n(\omega_c)] e^{i\omega_c t} - n(\omega_c) e^{-i\omega_c t} \} \right\} \quad (7a)$$

$$= N_e \exp \left\{ -\frac{\hbar^2 q_\perp^2}{2m^* \hbar \omega_c} \frac{1 + 2n(\omega_c)}{1} \right\} \sum_{l=0}^{\infty} \sum_{l'=0}^{\infty} \frac{[1 + n(\omega_c)]^l}{l!} \frac{[n(\omega_c)]^{l'}}{l'!} \left[\frac{\hbar^2 q_\perp^2}{2m^* \hbar \omega_c} \frac{1}{1} \right]^{l+l'} e^{i\omega_c t(l-l')}. \quad (7b)$$

If Eq. (7b) is substituted into Eq. (6), the time-integral I_t in Eq. (6) can be performed:

$$I_t = N_e \exp \left\{ -\frac{\hbar^2 q_\perp^2}{2m^* \hbar \omega_c} \frac{1 + 2n(\omega_c)}{1} \right\} \sum_{l=0}^{\infty} \sum_{l'=0}^{\infty} \frac{[1 + n(\omega_c)]^l}{l!} \frac{[n(\omega_c)]^{l'}}{l'!} \left[\frac{\hbar^2 q_\perp^2}{2m^* \hbar \omega_c} \frac{1}{1} \right]^{l+l'} \times \int_{-\infty}^{\infty} dt \{ [1 + n(\omega_q)] e^{it[\omega_c(l-l') + \omega_q]} - n(\omega_q) e^{it[\omega_c(l-l') - \omega_q]} \} \quad (8a)$$

$$= 2\pi N_e \exp \left\{ -\frac{\hbar^2 q_\perp^2}{2m^* \hbar \omega_c} \frac{1 + 2n(\omega_c)}{1} \right\} \sum_{l=0}^{\infty} \sum_{l'=0}^{\infty} \frac{[1 + n(\omega_c)]^l}{l!} \frac{[n(\omega_c)]^{l'}}{l'!} \left[\frac{\hbar^2 q_\perp^2}{2m^* \hbar \omega_c} \frac{1}{1} \right]^{l+l'} \times \{ [1 + n(\omega_q)] \delta(\omega_c(l-l') + \omega_q) - n(\omega_q) \delta(\omega_c(l-l') - \omega_q) \}. \quad (8b)$$

It is clear from Eqs. (6)–(8) that in the case of LO phonons ($\omega_q = \omega_{LO}$), $\mathbf{F}(\mathbf{v})$ and consequently also ρ_{xx} exhibit δ -function singularities as a function of the magnetic field at $n\omega_c = \omega_{LO}$ for $n = 1, 2, 3, \dots$. These singularities originate from the singular nature (i.e., series of δ functions) of the 2D density of states of free electrons in a magnetic field. In Refs. 5 and 6 it was argued that the singularities are damped by additional scattering with impurities, defects, acoustic phonons, etc., and the effect of these scattering processes was incorporated by replacing the δ functions by a Lorentz broadened form ($\delta(x) \rightarrow -(1/\pi) \text{Im}[1/(x + i\Gamma)]$). This Lorentzian broadening is equivalent to the inclusion of an exponential damping term, $e^{-\Gamma|t|}$, into the time integral of Eq. (2). In the present paper we will follow a different ap-

$$\mathbf{F}(\mathbf{v}) = \frac{2\beta}{N_e} \sum_{\mathbf{q}} \frac{\mathbf{q}(\mathbf{q} \cdot \mathbf{v})}{\hbar} |V_{\mathbf{q}}|^2 \text{Im}[D'(q, \omega_q)] \times n(\omega_q) [1 + n(\omega_q)] \quad (5)$$

with $\beta = 1/(k_B T)$.

This result, as obtained from the momentum-balance equation, leads to an expression for ρ_{xx} which is identical to the Kubo formula in the case of high magnetic fields. The Kubo formula³⁴ was the starting expression of the work of Lassnig and Zawadzki⁵ and of Vasileopoulos⁶ (in Ref. 6 inclusion of spin gives a multiplicative factor of 4).

The equivalent form for Eq. (5) in the time domain reads

$$\mathbf{F}(\mathbf{v}) = \frac{\beta}{N_e} \sum_{\mathbf{q}} \frac{\mathbf{q}(\mathbf{q} \cdot \mathbf{v})}{\hbar} |V_{\mathbf{q}}|^2 \times \int_{-\infty}^{\infty} dt \{ [1 + n(\omega_q)] e^{it\omega_q} - n(\omega_q) e^{-it\omega_q} \} S(\mathbf{q}, t). \quad (6)$$

From earlier work^{35,36} we know that for a nondegenerate electron gas in a magnetic field, $S(\mathbf{q}_\perp, t)$, where $\mathbf{q}_\perp \perp \mathcal{B}$, is given by

proach. A Gaussian broadening of the electron density of states will be adopted. Gerhardt²⁸ showed that a Gaussian broadening is obtained when the propagator of the free electron is taken to be $e^{[-iE_n t/\hbar - (\Gamma t)^2/8]}$ which results in a factor $e^{-(\Gamma t)^2/4}$ in the time integral of Eq. (2). We will take $\Gamma(\mathcal{B}) = (2\hbar\omega_c \Gamma_0/\pi)^{1/2}$ with Γ_0 a parameter, which, for convenience, is taken independent of the Landau-level index n . This is rigorous for short-range scatterers at zero temperature in high magnetic fields.³⁷ Motivated by the recent experiments on the 2D density of states, we will include a phenomenological flat background term in the density of states. Consequently, the 2D density of states is given by

$$D(E) = \frac{1}{2\pi l^2} \left[(1 - X_{BG}) \sum_{n=0}^{\infty} \left[\frac{2}{\pi} \right]^{1/2} \frac{1}{\Gamma_G} \exp \left[-\frac{2}{\Gamma_G^2} [E - (n + \frac{1}{2})\hbar\omega_c]^2 \right] + X_{BG} \frac{\Theta(E)}{\hbar\omega_c} \right], \quad (9)$$

with $\Theta(x)$ the Heaviside step function and X_{BG} the percentage of background states in the density of states.

Figure 1 displays the density of states at $\mathcal{B} = 20$ T for a Gaussian form with and without background (BG) and also for a Lorentzian broadening. The widths of the Lorentzian Γ_L and of the Gaussian Γ_G are taken such that they result in the same full width at half maximum for both types of broadening. The values of Γ_L and Γ_G at $\mathcal{B} = 20$ T are given in Fig. 1. Notice the similarity of the Lorentz form and the Gaussian with background.

For polar LO phonons $\omega_q = \omega_{LO}$ and $|V_q|^2 = 2\sqrt{2}\pi\alpha/(q^2\mathcal{V})$ in units $\hbar = m^* = \omega_{LO} = 1$ and with \mathcal{V} the crystal volume. For the quasi-2D EG in a single-interface GaAs heterostructure we will assume only the lowest electric subband is occupied, which will be described by the Fang-Howard²³ variational wave function $\Psi_{FH}(z) = 2^{-1/2} b^{3/2} z e^{-bz/2}$ with $b = [48\pi N e^2 / (m^* \hbar^2 \epsilon_s)]^{1/3}$. Here $N = N_d + \frac{11}{32} N_e$ with N_e, N_d the electron- and depletion-charge density, respectively. The interaction matrix element now contains a factor³⁸

$$\mathcal{J}_q = \sum_{\mathbf{q}} |V_{\mathbf{q}}|^2 I(q_z) \quad (10a)$$

with

$$\begin{aligned} \mathcal{J}(q_z) &= \left| \int_0^\infty dz |\Psi_{FH}(z)|^2 e^{iq_z z} \right|^2 \\ &= \left[1 + \left(\frac{q_z}{b} \right)^2 \right]^{1/3} \end{aligned}$$

and where $\mathbf{q}(q_x, q_z)$ is a three-dimensional vector and $\mathbf{q}_\perp(q_x, q_y)$ is a two-dimensional vector in the plane of the

2D EG. This sum \mathcal{J}_q in Eqs. (3b) and (5) can be rewritten by application of the continuum approximation. The q_z integral can be performed, due to the absence of dispersion of the LO phonons,

$$\mathcal{J}_q = \frac{\alpha}{2\sqrt{2}\pi} \int d^2(\mathbf{q}_\perp) \frac{\mathcal{F}(q_\perp)}{q_\perp} \quad (10b)$$

with the form factor $\mathcal{F}(x)$ given by

$$\mathcal{F}(x) = \begin{cases} 1 & \text{for the ideal 2D EG} \\ \frac{1}{8} \left[\frac{3}{1+x/b} + \frac{3}{(1+x/b)^2} + \frac{2}{(1+x/b)^3} \right] & \text{for the quasi-2D EG} \end{cases} \quad (11)$$

For the 2D EG interacting with LO phonons and when we take the density of states as Gaussians with a flat background, we find, from Eq. (5), for the linear magnetoresistance,

$$\bar{\rho}_{xx} = \frac{\rho_{xx}}{\rho_0^{\text{LO}}} = \frac{\alpha\tilde{\beta}}{8\pi\tilde{\Gamma}N_e} \tilde{\omega}_c^{5/2} [1 + n(\omega_{LO})] \sum_{n,m=0}^{\infty} I_x^{n,m} I_E^{n,m}, \quad (12)$$

where the tilde indicates that dimensionless units are used [e.g., $\tilde{\mathbf{v}} = \mathbf{v}/v_{LO}$ with $v_{LO} = (2\hbar\omega_{LO}/m^*)^{1/2} = 2^{1/2}$] and where

$$I_x^{n,m} = \int_0^\infty dx x^{1/2} J_{n,m}(x) \mathcal{F}(x/a),$$

$$\begin{aligned} I_E^{n,m} &= \frac{\tilde{\Gamma}}{2n(\omega_{LO})} \int_{-\infty}^\infty dE [f(E) - f(E-1)] \left[(1 - X_{BG}) \exp \left[-\frac{2}{\tilde{\Gamma}^2} (E + 1 - E_n)^2 \right] \right. \\ &\quad \left. + X_{BG} \left[\frac{\pi}{2} \right]^{1/2} \frac{\tilde{\Gamma}}{\tilde{\omega}_c} \Theta(E+1) \Theta(E+1-E_n) \Theta(E_{n+1}-1-E) \right] \\ &\quad \times \left[(1 - X_{BG}) \exp \left[-\frac{2}{\tilde{\Gamma}^2} (E - E_m)^2 \right] + X_{BG} \left[\frac{\pi}{2} \right]^{1/2} \frac{\tilde{\Gamma}}{\tilde{\omega}_c} \Theta(E) \Theta(E-E_m) \Theta(E_{m+1}-E) \right], \end{aligned}$$

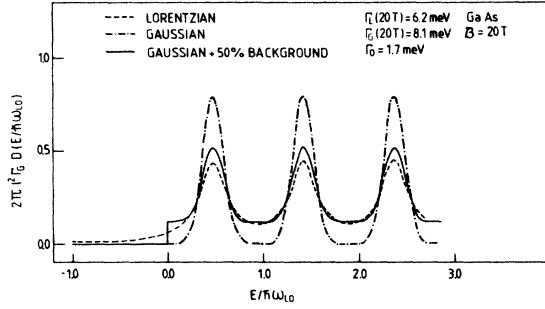


FIG. 1. Density of states of a two-dimensional electron gas in a perpendicular magnetic field of 20 T. Three types of Landau-level broadening are displayed: Lorentzian, Gaussian, and Gaussian with a flat background.

and where the resistivity is normalized to $\rho_0^{\text{LO}} = m^* \omega_{\text{LO}} / (N_e e^2)$,

$$\mathcal{F}(x) = \frac{1}{8} [3/(1+x^{1/2}) + 3/(1+x^{1/2})^2 + 2/(1+x^{1/2})^3]$$

is the form factor, $a = 2\bar{\omega}_c / \{[1 + 2n(\bar{\omega}_c)]b^2\}$, and $\beta = \beta \hbar \omega_{\text{LO}}$. The energies $E_n = (n + \frac{1}{2})\bar{\omega}_c$, $\bar{\omega}_c$, and $\bar{\Gamma}_G$ are in units of $\hbar \omega_{\text{LO}}$ ($\bar{\omega}_c = \hbar \omega_c / \hbar \omega_{\text{LO}}$). For a nondegenerate electron gas, the energy integral in $I_E^{n,m}$ can be performed explicitly, which, in the limit of zero background, results in

$$\begin{aligned} \bar{\rho}_{xx} = & \sqrt{\pi} \frac{\alpha \bar{\beta}}{\bar{\Gamma}} \bar{\omega}_c^{3/2} n(\omega_{\text{LO}}) (1 - e^{-\beta \bar{\omega}_c}) \\ & \times \sum_{n,m=0}^{\infty} I_x^{n,m} \exp \left[- \left| \frac{E_n - E_m - 1}{\bar{\Gamma}} \right|^2 \right. \\ & \left. + \frac{\bar{\beta}}{2} (1 - E_m - E_n) - \frac{(\bar{\beta} \bar{\Gamma})^2}{16} \right]. \end{aligned} \quad (13)$$

The last term in the exponential of Eq. (13) will cause a significant shift of the magnetophonon resonance peak positions if Γ is not much smaller than $k_B T$. The dependence of ρ_{xx} on the parameters T , Γ_0 , and BG is studied in Fig. 2, where $\rho_{xx}(B)/\rho_0$ is shown as a function of $\omega_{\text{LO}}/\omega_c$ for the ideal 2D EG. For the numerical results presented in this paper, material constants are taken for GaAs; i.e., $m^*/m_e = 0.07$ and $\hbar \omega_{\text{LO}} = 36.6$ meV. It appears from Fig. 2(a) that ρ_{xx} is very sensitive to the temperature T when $T < 140$ K. At resonance it increases steeply with T . For $140 < T < 300$ K, on the other hand, the oscillations in ρ_{xx} are largest around 200 K, but ρ_{xx} is rather insensitive to T . The oscillations in ρ_{xx} persist at least up to $T = 300$ K, which agrees with experimental observations of Englert *et al.*¹⁰ This is very much like the 3D case, where magnetophonon resonance oscillations are observable² up to 350 K for GaAs. However, the maximum amplitude of the magnetophonon oscillations in ρ_{xx} in bulk GaAs is observed² at lower temperature (140 K) as compared to the 2D case. Notice that the peak position of the magnetophonon resonances are shifted to the lower magnetic field side and that this shift

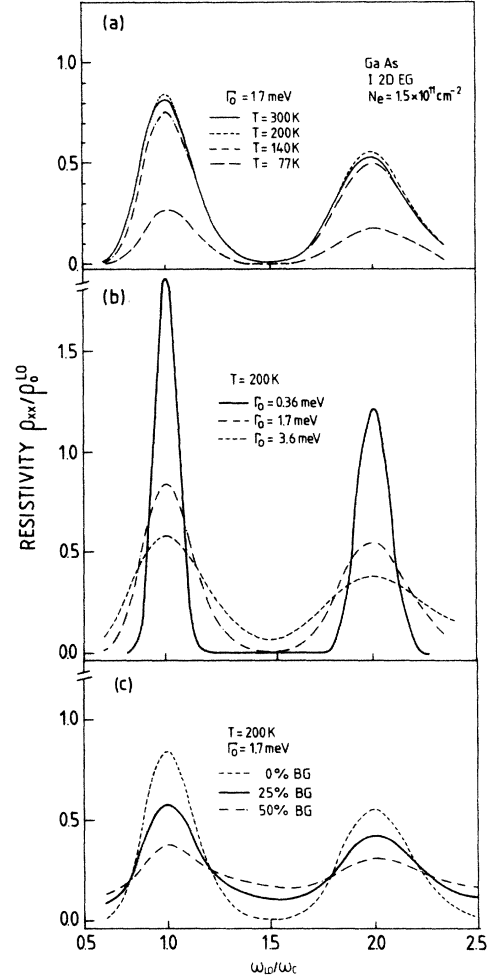


FIG. 2. The linear transverse resistivity of the ideal two-dimensional electron gas as a function of $\omega_{\text{LO}}/\omega_c$, for different values of the parameters: (a) temperature (T), (b) broadening (Γ_0), and (c) background (% BG).

increases with decreasing temperature. We checked that up to $N_e = 5 \times 10^{11} \text{ cm}^{-2}$, ρ_{xx} coincides (within a 1% level) with the Boltzmann case. This implies that the exclusion principle does not play a significant role here. Figure 2(b) indicates that ρ_{xx} is sensitive to the value of Γ , both at resonance ($n \omega_c = \omega_{\text{LO}}$) and far from it. The effect of a flat background is to smoothen out the magnetophonon resonances and to increase ρ_{xx} appreciably between the resonance maxima. Both the Gaussian broadening and the background shift the peak positions to lower magnetic fields. The shift increases with increasing Γ_0 and background percentage and it decreases with increasing temperature. At 200 K and for a fixed background of 25%, the relative shift of the $n=1$ peak position is 1.0%, 2.0%, 3.5%, and 5.0% for $\Gamma_0 = 0.9, 1.7, 3.6$, and 5.2 meV, respectively. At 200 K and for a fixed $\Gamma_0 = 3.6$ meV this relative shift amounts to 2.0%, 3.5%, and 5.5% for a background of 0%, 25%, and 50%, respectively, while for fixed $\Gamma_0 = 1.7$ meV and 25% background states, we find a relative shift of 1.0%, 1.6%, 2.4%, 3.2%, 4.0%, and 5.0% at temperatures of 300, 200, 150, 130, 100, and 77 K, respectively.

Next we will compare the present model with the experimental results of Englert *et al.*¹⁰ and with the theoretical results of Lassnig and Zawadzki⁵ where a Lorentzian broadening was assumed (see lower part of Fig. 3). The upper part of Fig. 3 displays ρ_{xx}/ρ_0 as a function of B , where ρ_0 is the experimental low-field resistivity. The values of the parameters are chosen identical to those given in the paper of Lassnig and Zawadzki⁵ (except for the background). The curve with zero background obviously shows too large magnetophonon resonance amplitudes. On the other hand, the curve with 25% background describes the experimental results reasonably well and agrees with the results of Lassnig and Zawadzki⁵ for the $n=1$ and 2 peaks. The magnetophonon resonance amplitudes for 25% background at magnetic fields below 10 T ($n=3,4$) are more pronounced than for the Lorentzian broadening approach. For both types of broadening the peak positions are shifted relative to the magnetic field for which $\omega_c = \omega_{LO}$. For the Lorentzian broadening of Ref. 5 the $n=1$ peak position is shifted $\approx 3\%$ to the higher magnetic fields, as opposed to the present results for Gaussian broadening with 25% background which show a shift of approximately 2% to lower magnetic fields. The two different types of broadening lead to magnetophonon resonance peak shifts which have opposite sign.

In order to estimate the effect of a nonparabolic energy-momentum relation on the magnetophonon resonances, the Landau-level energies $E_n = (n + \frac{1}{2})\hbar\omega_c$ in Eq. (12) were replaced by the nonparabolic energies as obtained from a three-band Kane theory as presented in

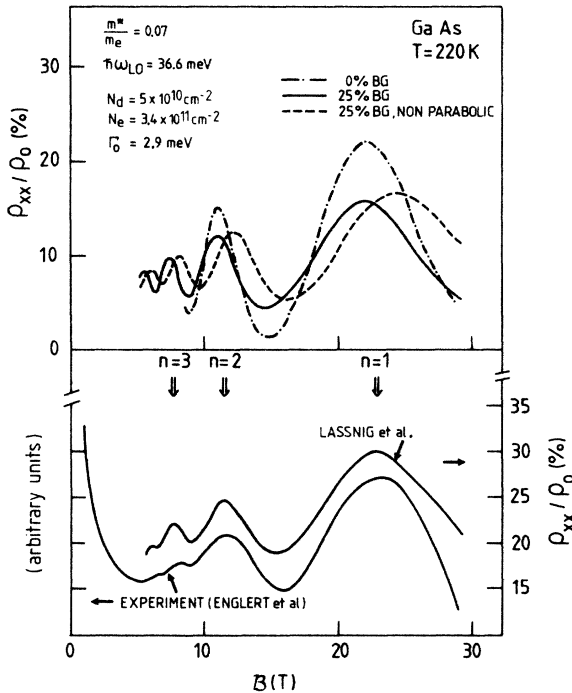


FIG. 3. Comparison of the present theory for the linear transverse resistivity with the experiment of Englert *et al.* (Ref. 10) and the theory of Lassnig and Zawadzki (Ref. 5) at $T = 220 \text{ K}$. The parameters and material constants are taken from Ref. 5.

Ref. 39. The energy gap and the static dielectric constant were taken to be equal to 1.457 eV and 12.8, respectively (see Ref. 40). The results are shown in the upper part of Fig. 3. Two effects are present: (1) a small shift of the whole curve to higher resistivities and (2) a shift of the magnetophonon resonance peak positions to larger magnetic fields, which amounts to about 10% for the $n=1$ peak as compared to the case for parabolic bands (solid curve in the upper part of Fig. 3). The fundamental resonance ($n=1$) appears at 24.1 T, which is approximately 7% larger than the value obtained from experiment in Ref. 10 ($22.5 \pm 0.5 \text{ T}$). Therefore the effective electron mass seems to be somewhat smaller than $0.07m_3$, if we take $\hbar\omega_{LO}$ equal to the bulk GaAs energy, the validity of which was recently discussed in Ref. 14. The calculation of Lassnig and Zawadzki⁵ with Lorentzian broadening would lead to a still smaller effective mass, since the shift of the $n=1$ peak position due to the broadening seems to be relatively large and adds to the shift due to nonparabolicity (both have the same sign).

Both the present calculation and the calculations of Refs. 5 and 6 give a contribution of the electron-phonon interaction to ρ_{xx} which does not vanish at any B . The experimental results usually display only the oscillatory part of the resistivity $\Delta\rho_{xx}/\rho_0$, where ρ_0 is the zero magnetic field resistivity and where $\Delta\rho_{xx}$ is obtained by subtracting the nonoscillatory part (so-called "background contribution") of ρ_{xx} . In doing so, the nonoscillatory contribution of the LO-phonon scattering cannot be measured separately, because contributions from impurity scattering, etc. are also present. In order to compare the present calculation with that of Vasilopoulos⁶ we tried to fit Eq. (3.14) of Ref. 6 to the experimental results of Ref. 10. However, the values for the layer width L_z and the broadening parameter Γ_0 which were needed are an order of magnitude larger than those taken in the theories which are presented in Fig. 3. Thus in Ref. 6 the magnitude of the magnetophonon oscillations is severely overestimated.

IV. ELECTRON TEMPERATURE MODEL

For the study of nonlinear effects, we will first adopt a simple electron temperature model. This is the simplest model to describe nonlinear transport phenomena and it is often useful in the analysis of experimental data. As it is difficult to know *a priori* how quantitatively accurate its results will be,³ detailed comparison with experimental data could shed some light on the validity of such a model. The electronic response is still given by the linear expression but the electron energy distribution is taken to be a heated Fermi or Boltzmann function (in the nondegenerate case) with an electron temperature $T_e \neq T(\text{lattice})$. It is equivalent to the evaluation of ρ_{xx} with $S(\mathbf{q}, t)$ in Eq. (5) calculated at $T_e \neq T$. Figure 4 (lower part of the figure) displays the amplitudes of the magnetophonon resonance peaks $n=1, 2, 3$ as a function of electron temperature at a fixed lattice temperature of 77 K. The amplitude is defined as $[\rho_{xx}(\text{max}) - \rho_{xx}(\text{min})]/\rho_0^{LO}$. In the upper part of the figure, the amplitudes are displayed, relative to the amplitude at

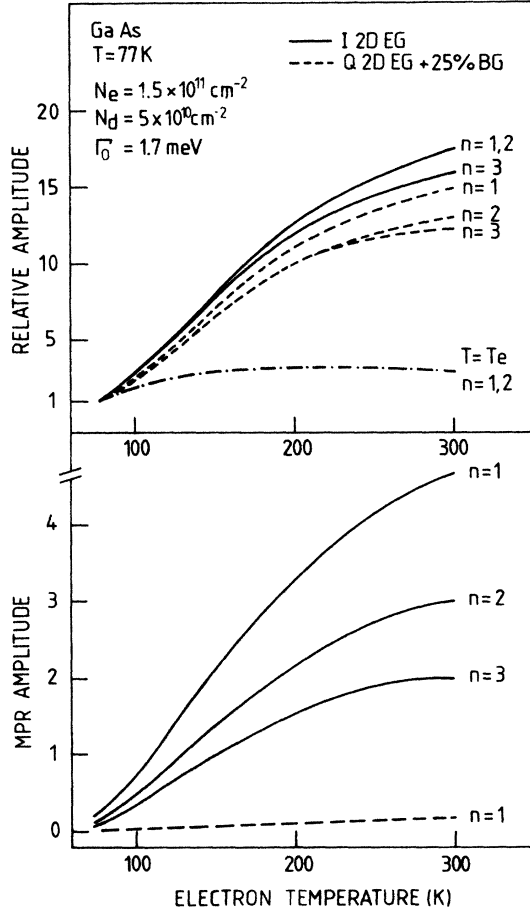


FIG. 4. Amplitudes of the magnetophonon resonance peaks $n=1,2,3$ as a function of the electron temperature at a lattice temperature $T=77$ K. The amplitudes are defined as $[\rho_{xx}(\max) - \rho_{xx}(\min)]/\rho_0^{\text{LO}}$. In the upper part of the figure, the amplitudes are displayed relative to the amplitude at $T=T_e=77$ K for the ideal 2D EG as well as the quasi-2D EG with 25% background. For comparison a curve with $T_e=T$ is also given.

$T=T_e=77$ K. The curves for the ideal 2D EG (I 2D EG) and the quasi-2D EG (with 25% background) and for different resonances n all show the same trend: an increase of the relative amplitude with increasing T_e . The effect of increasing T_e at fixed T is much stronger than the effect of increasing T such that $T=T_e$ (see the dash-dotted curve). This shows that 2D EG hot-electron magnetophonon resonances at low lattice temperatures potentially have larger amplitudes than the normal magnetophonon resonances at high lattice temperatures. As a consequence, the magnetophonon resonance effect is better studied at low lattice temperature, but with a heated 2D EG. This is similar to the 3D case. The amplitude of the magnetophonon resonance peaks $n=1-4$, normalized to experimental resistivity at $B=0$ (ρ_0), is plotted in Fig. 5 for the experimental quasi-2D EG of Ref. 10 at a lattice temperature $T=4.2$ K. For $T_e < 40-50$ K the magnetophonon resonance amplitudes are below the 1% level. On the other hand, for T_e around 100 K they become of the same order of magni-

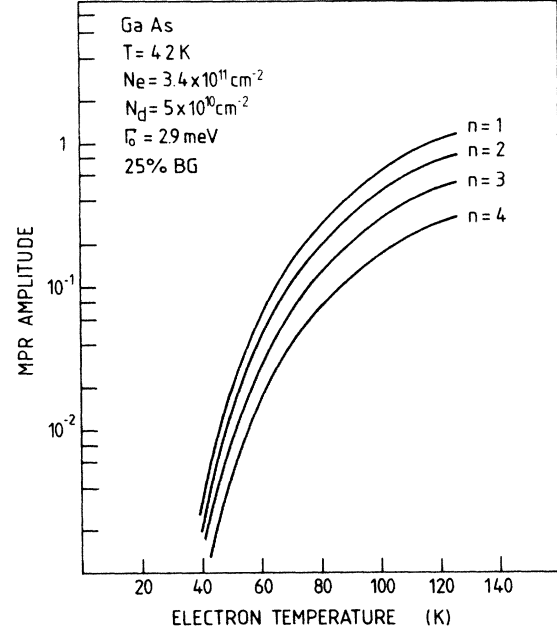


FIG. 5. Amplitudes of the magnetophonon resonance peaks $n=1-4$ as a function of electron temperature at $T=4.2$ K, defined as $[\rho_{xx}(\max) - \rho_{xx}(\min)]/\rho_0$ where ρ_0 is the experimental resistivity at $B=0$. The densities are for the single-interface heterojunction of Ref. 10.

tude as ρ_0 . Thus on the basis of these results we find $T_e=40$ K as the lower limit for the observation of hot-electron magnetophonon resonances at a lattice temperature of 4.2 K. This is in agreement with the experimental work of Sakaki *et al.*,¹⁶ who studied the effect of heating of the 2D EG in GaAs-Al_xGa_{1-x}As heterostructures on Shubnikov-de Haas oscillations at 4.2 K. When $T_e > 40$ K they observe extra peaks in the resistivity, which they attribute to resonant emission of LO phonons.

Another important quantity for hot-electron transport is the energy transfer rate from the electrons to the lattice. This quantity is most easily obtained from the energy-balance equation. The energy transfer rate for an electron with average velocity v is

$$W(v) = \frac{1}{N_e} \sum_q \frac{\omega_q}{\hbar} |V_q|^2 \times \int_{-\infty}^{\infty} dt \{ [1 + n(\omega_q)] e^{it(\omega_q - q \cdot v)} - n(\omega_q) e^{-it(\omega_q - q \cdot v)} \} S(q, t), \quad (14a)$$

or equivalently

$$W(v) = \frac{2}{N_e} \sum_q \frac{\omega_q}{\hbar} |V_q|^2 \text{Im}[D'(q, \omega_q - q \cdot v)] \times [n(\omega_q) - n(\omega_q - q \cdot v)]. \quad (14b)$$

Within the electron temperature model only terms up to order v^0 are retained in the expression for the energy relaxation rate. In this model one assumes a heated but unshifted Fermi function for the electron energy distribution function. Within this approximation the energy relaxation rate (in units of W/electron) is given by

$$W = 2.4342 \times 10^{-10} [\hbar\omega_{LO} \text{ (meV)}]^2 \frac{\alpha \tilde{\omega}_c^{3/2} n(\omega_{LO})}{2\pi \tilde{\Gamma} N_e} \times (e^{\beta_e} - e^{\beta}) \sum_{n,m=0}^{\infty} I_E^{n,m} J_x^{n,m} \quad (14c)$$

with

$$J_x^{n,m} = \int_0^{\infty} dx x^{-1/2} J_{n,m}(x) \mathcal{F}(x/a)$$

and $\beta_e = \hbar\omega_{LO}/(k_B T_e)$ the inverse electron temperature. In the limit of zero background in the electron density of states and in the case of a nondegenerate electron gas (Boltzmann statistics) Eq. (14c) reduces to

$$W = 2.4342 \times 10^{-10} [\hbar\omega_{LO} \text{ (meV)}]^2 \frac{\alpha}{\tilde{\Gamma}} (\pi \tilde{\omega}_c)^{1/2} \times (1 - e^{\beta \tilde{\omega}_c}) \frac{(1 - e^{\beta - \beta_e})}{(1 - e^{\beta})} \times \sum_{n,m=0}^{\infty} J_x^{n,m} \exp \left[- \left(\frac{E_n - E_m - 1}{\tilde{\Gamma}} \right)^2 + \frac{\tilde{\beta}}{2} (1 - E_m - E_n) - \frac{(\tilde{\beta} \tilde{\Gamma})^2}{16} \right], \quad (15)$$

which is proportional to $e^{-\beta_e}$ when $T_e \gg T$ and to $e^{-\beta(T_e - T)/(TT_e)}$ when $T_e \approx T$ and for low temperatures. This exponential behavior is clearly apparent in the curves of Fig. 6. Curves for different values of the fixed magnetic field are labeled with the corresponding value of the inverse magnetic field ω_{LO}/ω_c . These results mirror the fact that the energy relaxation rate also shows magnetophonon resonances. The inclusion of the nonzero width of the 2D layer results in an overall reduction of the magnitude of the energy relaxation rate by an order of magnitude, but does not lead to a broadening of the magnetophonon oscillations in the energy relaxation rate, as is apparent from Fig. 7. The effect of different values for Γ_0 and of a nonzero background term on these oscillations in the energy relaxation rate is displayed in Fig. 7: the whole oscillatory structure is smeared out, and the background term predominantly fills up the valleys, but also shifts the peak positions to slightly lower magnetic fields. On the average the amplitude of the oscillations in the energy relaxation rate decreases with decreasing magnetic field. The energy relaxation rate is rather sensitive to the broadening parameters, as can be observed from Table I, which summarizes the data of Fig. 7 for the $n=1$ peak. Over the range of realistic values for these parameters, the largest and smallest amplitude in the energy relaxa-

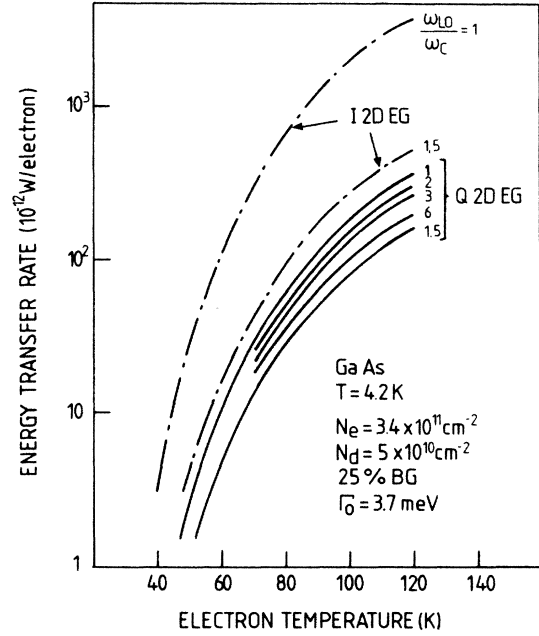


FIG. 6. Energy transfer rate for ideal 2D EG and quasi-2D EG as a function of electron temperature at $T = 4.2$ K. The numbers at the curves are values for ω_{LO}/ω_c .

tion rate differ by a factor of 4.

Hollering *et al.*⁴¹ measured the time τ_{eff} for electrons (and holes) to cool down to $T_e = 100$ K at a lattice temperature of 4.2 K. These experimental results show τ_{eff} as a function of \mathcal{B} , but with a very large step in \mathcal{B} , so that magnetophonon resonance oscillations in $\tau_{\text{eff}}(\mathcal{B})$ could certainly not be resolved if they were present at all. From $\mathcal{B} = 0-8$ T τ_{eff} increases and then decreases from 8 to 20 T. These results were confirmed by the measurements of Ryan *et al.*,⁴² which show a maximum in the cooling time around 9 T. This would mean that the energy relaxation rate has a minimum around 9 T. Our present results indicate that LO-phonon scattering alone cannot explain these experimental results. Hollering *et al.*⁴¹ attributed the decrease in τ_{eff} for $\mathcal{B} > 9$ T to interaction with acoustic phonons, while Ryan *et al.*⁴² suggest that hole relaxation induces a maximum in the cooling time. In our opinion this behavior is still not completely explained. Work is in progress to include acoustic-phonon scattering in our calculations, which will allow a comparison with Refs. 41 and 42.

V. THE NONLINEAR REGIME

The nonlinear momentum-balance equation will be solved here for the case of Boltzmann statistics. From the foregoing sections we know that the effect of the exclusion principle on the magnetophonon resonances is very small for the considered experimental situation (temperatures $T > 60$ K, electron densities $N_e < 5 \times 10^{11}$ cm⁻² and magnetic fields greater than 8 T). We will assume that the electron temperature equals the lattice

temperature. In principle one should solve the coupled set of momentum- and energy-balance equations. We believe that the results of the present model will show the correct qualitative trends. Although there is some experimental evidence for a heating of the phonon population²² at zero magnetic field, we assume thermal equilibrium for the LO-phonon distribution.

librium for the LO-phonon distribution.

For convenience (limiting the CPU time), the flat background part of the density of states will be neglected. This will result in more pronounced oscillations. Performing the energy integral in Eq. (3b), one arrives at a numerically tractable form,

$$\begin{aligned} \tilde{F}(\bar{v}) = & 4 \left(\frac{2}{\pi} \right)^{1/2} \frac{\alpha}{\tilde{\Gamma}} n(\omega_{LO}) (1 - e^{-\beta \tilde{\omega}_c}) \sum_{n,m=0}^{\infty} \exp \left[- \left(\frac{E_n - E_m - 1}{\tilde{\Gamma}} \right)^2 + \frac{\tilde{\beta}}{2} (1 - E_m - E_n) - \frac{(\tilde{\beta} \tilde{\Gamma})^2}{16} \right] \\ & \times \int_0^{\infty} dx J_{n,m}(x) \mathcal{F}(x/a) \\ & \times \int_0^1 dy \cosh \left[\frac{2\bar{v}}{\tilde{\Gamma}^2} (1 + E_m - E_n) [x(1-y^2)]^{1/2} \right] \\ & \times \sinh \left[\tilde{\beta} \bar{v} \left(\frac{\tilde{\omega}_c}{2} x(1-y^2) \right)^{1/2} \right] \exp \left[\frac{2\tilde{\omega}_c \bar{v}^2}{\tilde{\Gamma}^2} x(y^2 - 1) \right]. \end{aligned} \quad (16)$$

The nonzero velocity changes the resonance condition such that a \mathbf{q} -dependent term, i.e., $\mathbf{q} \cdot \mathbf{v}$, is included which will broaden and shift the magnetophonon resonance peaks. This term will remove the δ -function singularities even for $\Gamma_0 = 0$, as was recently pointed out by Horing *et al.*⁴³ In the limit of extremely large velocity $\mathbf{F}(\mathbf{v})$ vanishes for all T and \mathcal{B} , which expresses runaway of the electrons.

Recently Vasilopoulos *et al.*⁷ analyzed nonlinear transport in 2D quantum wells. They found (1) that the linear conductivity σ_{xy} depends on the layer thickness and on temperature, (2) magnetophonon resonance maxima in σ_{xx} convert into minima at sufficiently high electric fields (see also below), and (3) oscillations are present due to inter-electric-subband scattering. Here only the lowest electric subband is considered. They make the following approximations: (1) small electron-phonon coupling, (2) a Maxwellian electron distribution function, (3) replace the microscopic conservation of energy $\delta(x_0)$

by a Lorentzian form, (4) neglect the q_z dependence of the electron-phonon interaction coefficient V_q , (5) replace $\mathbf{q} \cdot \mathbf{v}$ by $e\mathcal{E}\Delta x$ with Δx a constant of order 1, and (6) assume a nonequilibrium phonon temperature. Approximations (1) and (2) are the same as in the present model. We do not make approximations (3), (4), and (5) but will calculate the equations exactly, although numerically. In our calculation the LO-phonon distribution is taken to be in equilibrium [point (6)]. Unfortunately, no numerical results were given in Ref. 7 so that a detailed comparison of the two models is not possible.

For the warm-electron regime we will look at the first derivative of ρ_{xx} with respect to the electric field. Therefore we expand Eq. (16) up to order v^3 and write it in the form

$$\tilde{F}(\bar{v}) = A_0 \bar{v} + A_1 \bar{v}^3, \quad (17)$$

with

$$A_0 = \tilde{\rho}_{xx}(v=0),$$

$$\begin{aligned} A_1 = & \frac{3}{8} \sqrt{\pi} \frac{\alpha \tilde{\beta}}{\tilde{\Gamma}} n(\omega_{LO}) \tilde{\omega}_c^{5/2} (1 - e^{-\beta \tilde{\omega}_c}) \sum_{n,m=0}^{\infty} \exp \left[- \left(\frac{E_n - E_m - 1}{\tilde{\Gamma}} \right)^2 + \frac{\tilde{\beta}}{2} (1 - E_m - E_n) - \frac{(\tilde{\beta} \tilde{\Gamma})^2}{16} \right] \\ & \times \int_0^{\infty} dx J_{n,m}(x) \mathcal{F}(x/a) x \left[\frac{\tilde{\beta}^2}{6} - \frac{4}{\tilde{\Gamma}^2} + \frac{8}{\tilde{\Gamma}^4} (E_n - E_m - 1) \right], \end{aligned}$$

and where the limit of zero background is taken.

Near resonance, the term $8(E_n - E_m - 1)/\tilde{\Gamma}^4$ in the last expression in large parentheses of A_1 is very small and consequently, A_1 is negative (ρ_{xx} decreases with the electric field \mathcal{E}) when $\Gamma \ll 5k_B T$, i.e., for high temperatures and small Γ . Far from resonance A_1 is positive

(ρ_{xx} increases with \mathcal{E}). This is again similar to the 3D case.^{2,3} The magnitude and the sign of A_1 are apparently very sensitive to the value of Γ . The magnetic field dependence of A_1 is shown in Fig. 8 for the ideal 2D EG at $T = 200$ K and for various values of Γ_0 and background percentage. One observes that (1) for a back-

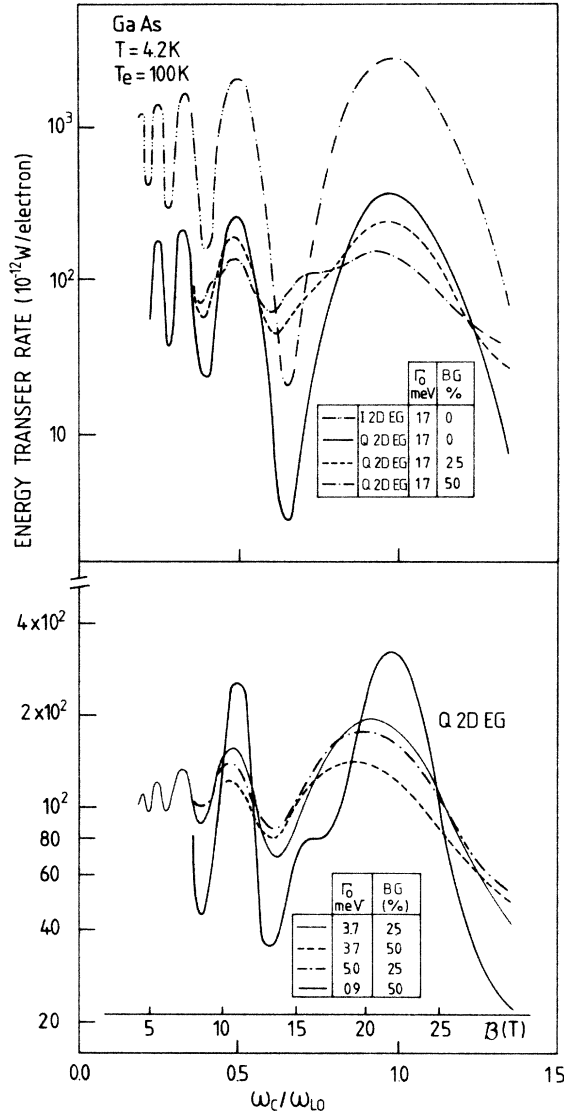


FIG. 7. Energy transfer rate for ideal 2D EG and quasi-2D EG as a function of ω_{LO}/ω_c at $T=4.2$ K and $T_e=100$ K. The equivalent scale of the magnetic field is indicated. In (a) the BG is changed, while in (b) both Γ_0 and BG are varied.

ground of $\geq 25\%$, A_1 is never negative, (2) the background term has a large overall effect and, i.e., it increases A_1 and it induces a shift in the position of the main minima, and (3) an additional structure (maximum, minimum, maximum) between the main minima at resonance is found. This additional structure originates from the behavior of the dominant Gaussian terms (see inset of Fig. 8) and it is only pronounced for very narrow Landau levels (very pure samples).

Introducing a warm-electron coefficient β_v , which is an experimentally measurable quantity (see, e.g., Hamaguchi *et al.*⁴⁴ for results of 3D conduction in InSb), the nonlinear resistivity $\rho_{xx}(v)$ can be written approximately as

$$\rho_{xx}(v) = \rho_{xx}(v=0)[1 + \beta_v \mathcal{E}_a^2], \quad (18a)$$

TABLE I. The amplitude of the $n=1$ magnetophonon resonance peak in the energy relaxation rate and the ratio of the $n=1$ maximum to the subsequent minimum for different values of the broadening parameters.

Γ_0 (meV)	Background (%)	Amplitude (10^{-10} W)	ρ_{\max}/ρ_{\min}
1.7	0	3.80	130
1.7	25	2.05	5.5
1.7	50	0.95	2.5
0.9	25	2.90	9.1
1.7	25	2.05	5.5
3.7	25	1.26	2.8
5.0	25	0.98	2.2

$$\tilde{\beta}_v = \frac{\beta_v}{\mathcal{E}_0} = \frac{A_1}{(A_0)^3}, \quad (18b)$$

with $\mathcal{E}_0 = m^* \omega_{LO} v_{LO} / e$ and \mathcal{E}_a the applied electric field. β_v as calculated from Eqs. (17) and (18) and using parameters for the quasi-2D EG of Ref. 10 is large (compared to typical values of β_v for 3D InSb at $T=77$ it is 10^4 times larger) and shows pronounced oscillations (see Fig. 9). This is due to the fact that we only take into account the electron LO-phonon contribution to A_0 . A_0 contains strong oscillations [$A_0 = \tilde{\rho}_{xx}(v=0)$] and consequently the oscillations in β_v are enhanced, through its

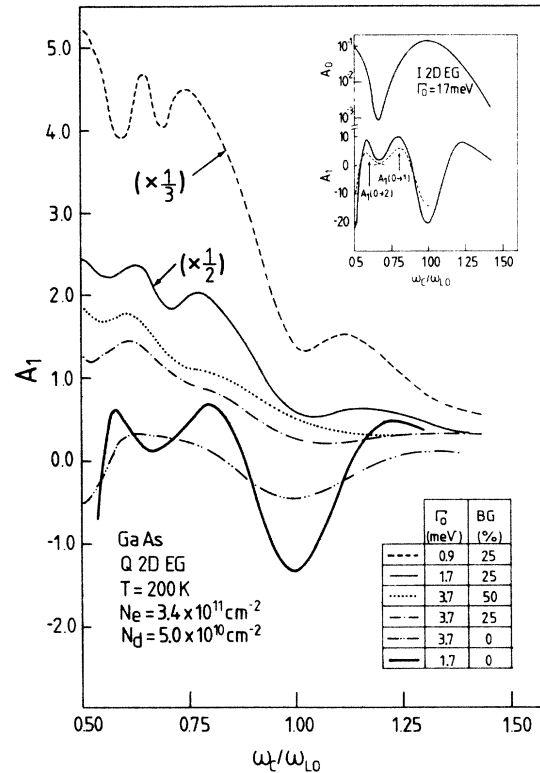


FIG. 8. Dependence on ω_{LO}/ω_c of the coefficient A_1 from Eq. (17), for the quasi-2D EG and for different values of Γ_0 and BG at $T=200$ K. The inset shows A_1 and A_0 for the ideal 2D EG with $\Gamma_0=1.7$ meV and no background. The dominant terms which contribute to A_1 are displayed in the inset.

strong dependence on A_0 [Eq. (16b)]. In reality, other processes like impurity scattering, acoustic-phonon scattering, etc. dominate the behavior of A_0 , while for the nonlinear coefficient A_1 this is much less the case. For $T \gg 40$ K the deviation of ρ_{xx} from the linear response is dominated by interaction with LO phonons. From Fig. 9 we observe that (1) on the average β_v increases with decreasing magnetic field and the oscillations in β_v rapidly die out when $\omega_c \ll \omega_{LO}$, (2) the addi-

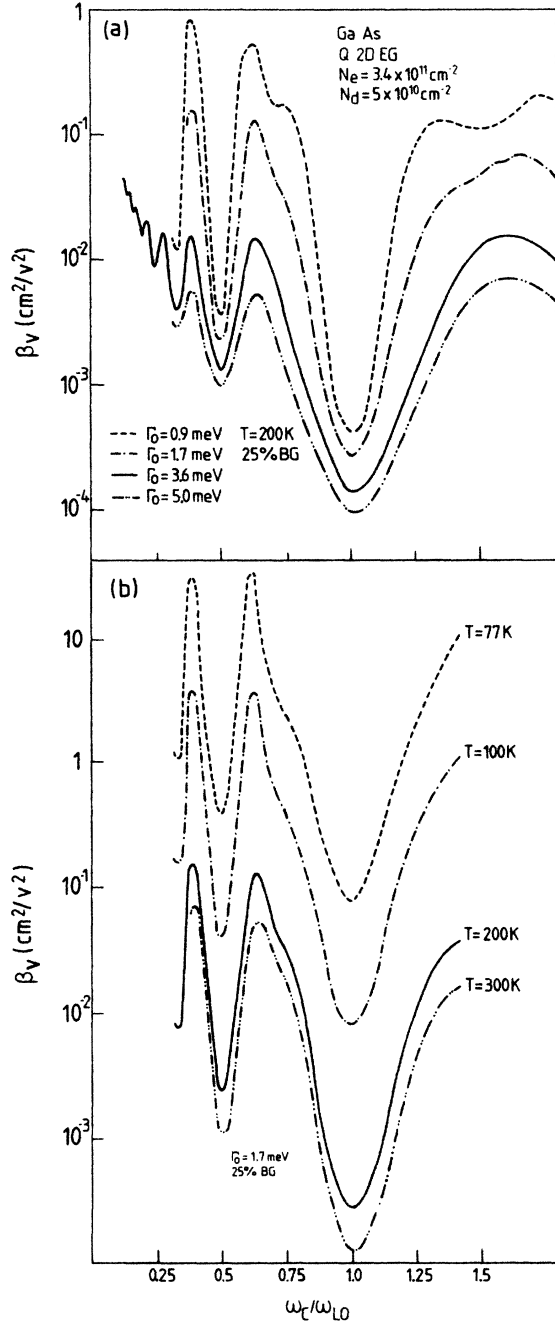


FIG. 9. Warm-electron coefficient [see Eq. (18)] as a function of ω_{LO}/ω_c for the quasi-2D EG at $T=200$ K. The upper part gives results for different values of Γ_0 and in the lower part of the figure for different temperatures.

tional structure in A_1 is reflected in β_v only when Γ is small, and (3) the influence of temperature is dramatic: roughly a factor of 100 decrease in β_v occurs as the temperature is increased from $T=77$ to 200 K.

Below we discuss the numerical results for general values of the average velocity as given by expression (16). The magnetophonon resonances in the nonlinear resistivity ρ_{xx}/ρ_0^{LO} for the quasi-2D EG are shown in Fig. 10 for different values of the average electron velocity (i.e., current density). The upper part of Fig. 10 shows results for $T=200$ K and the lower part for $T=77$ K. The same broadening parameters are taken for both temperatures. For small velocities ($v/v_{LO} < 0.1$) the extrema are shifted to the lower magnetic field side and the amplitudes of the oscillations decrease. For higher velocities ($v/v_{LO} > 0.1$) the resistivity shows maxima at those magnetic fields for which in the linear case it shows a minimum and similarly the maxima convert into minima. The oscillations are quite large, but it is expected that inclusion of a flat background term in the density of states will smoothen them substantially. We expect that the general qualitative trend will not be changed by the inclusion of the background term.

Figure 11 displays the shift in position of the $n=1$ maximum and of the subsequent minimum (i.e., at lower magnetic fields) as a function of the velocity (quasi-2D EG at $T=77$ and 200 K). The almost discontinuous change in the position of the minimum around $v/v_{LO}=0.1$ at $T=200$ K in fact marks the disappear-

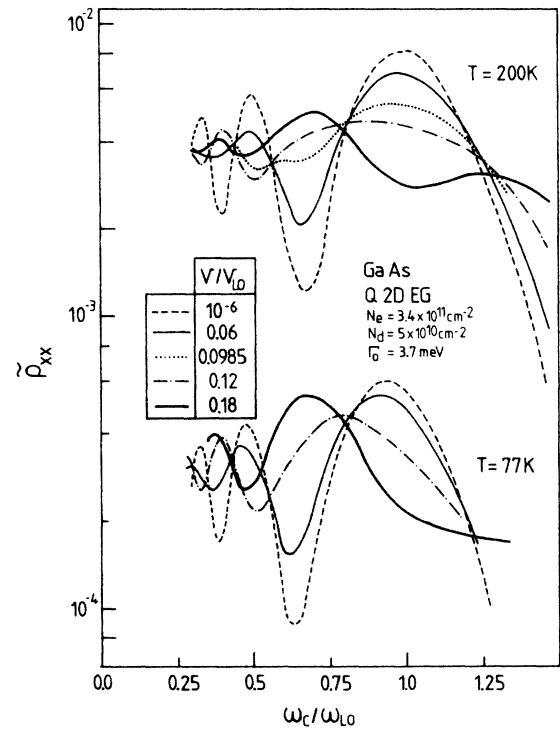


FIG. 10. The magnetic field dependence of the nonlinear resistivity $\bar{\rho}_{xx} = \rho_{xx}/\rho_0^{LO}$ [see Eq. (16)] for the quasi-2D EG with Gaussian broadening at a constant current density. The corresponding values for the velocity v/v_{LO} are given in Table I.

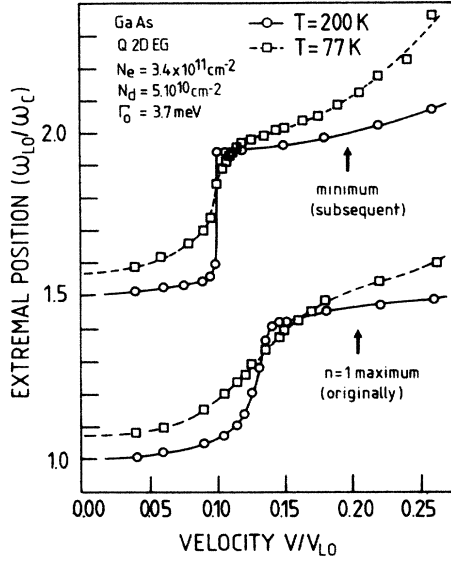


FIG. 11. The position of the maximum, which in the linear case is the $n=1$ magnetophonon resonance maximum, and the position of the subsequent minimum, both as a function of the velocity. Results are given for the quasi-2D EG at $T=77$ and 200 K, and the value of Γ_0 is kept constant. The curves are a guide to the eye.

ance of a minimum around $\omega_c \approx \omega_{LO}/1.5$ (see, in Fig. 10, the curve for $T=200$ K and $v/v_{LO}=0.0985$). Up to $v/v_{LO} < 0.1$, the shift of the position of the maximum away from the resonance condition $\omega_c \approx \omega_{LO}$ is small. Around $v/v_{LO}=0.1$ the position of the maximum shifts rapidly and then it is pinned around $\omega_c = \omega_{LO}/1.5$. A similar behavior can also be found in the shift of the position of the subsequent minimum which evolves from $\omega_c \approx \omega_{LO}/1.5$ when $v/v_{LO} < 0.1$ to $\omega_c \approx \omega_{LO}/2$ when $v/v_{LO} > 0.1$. The transition from a maximum to a minimum with increasing velocity occurs at smaller velocities when n is larger. This is apparent from Fig. 10 where for $v/v_{LO}=0.12$ the $n=1$ resonance is still a maximum, while the $n=2$ resonance is already transformed into a minimum.

The dependence of the nonlinear resistivity $\bar{\rho}_{xx} = \rho_{xx}/\rho_0^{LO}$ on the average velocity is displayed in Fig. 12 for the quasi-2D EG at $T=77$ and 200 K in a constant magnetic field. The scale on the right side gives values for ρ_{xx} normalized to the experimental values for ρ_0 of Ref. 10. For $B=21$ T, which is near the $n=1$ magnetophonon resonance in the linear case, ρ_{xx} decreases first with increasing velocity. It shows a minimum around $v/v_{LO}=0.2$ and for larger velocities it increases with v . For $B=14$ T, which is near to the minimum in the linear case, ρ_{xx} increases with v and attains a maximum around $v/v_{LO} \approx 0.2$ and a subsequent dip around $v/v_{LO} \approx 0.25$, followed by an increase. For $v/v_{LO} > 0.25$, ρ_{xx} (1) increases steeply for $T=77$ K, and (2) becomes almost independent of T and B (almost coincides with the results for $T=200$ K). This behavior can be interpreted as a saturation of the velocity near $v/v_{LO}=0.5$. As in the simple Shockley model the resistivity and thus also the applied electric field $\mathcal{E}_a \sim \rho_{xx} v$

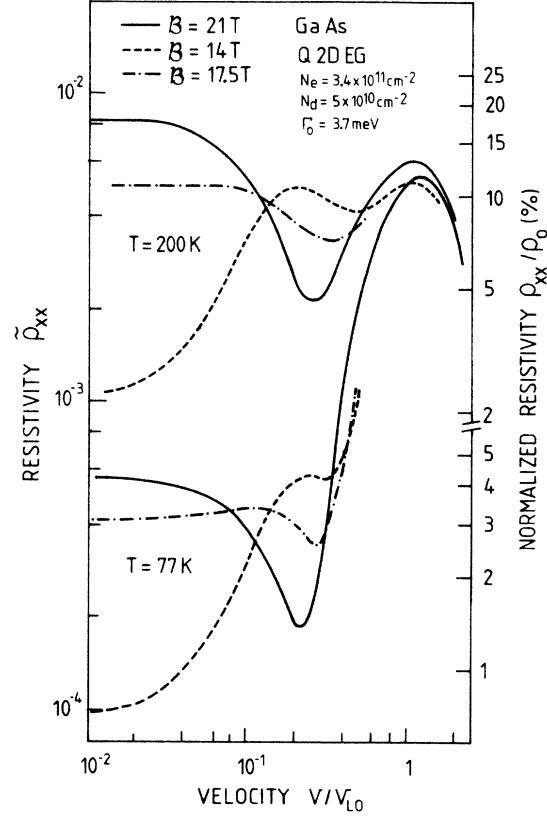


FIG. 12. The nonlinear resistivity ρ_{xx}/ρ_0^{LO} as a function of the average velocity for the quasi-2D EG at $T=77$ and 200 K. Results are displayed for different magnetic field values. The right scale gives values of ρ_{xx}/ρ_0 in percent, with ρ_0 from experiment.

increase steeply around $v/v_{LO}=0.5$, while the velocity is almost constant. For $v/v_{LO} > 1$ the resistivity decreases again and the “runaway” of the electrons sets in.

VI. CONCLUSIONS

In this paper magnetophonon oscillations were investigated in the linear and nonlinear electric field region for a two-dimensional electron gas subjected to crossed electric and magnetic fields. The following approximations were made: (1) we consider an effective-mass approximation for the electrons, (2) only the first electric subband is supposed to be populated, (3) screening is neglected, but Fermi-Dirac statistics is retained, (4) the phonons are considered to be in equilibrium with the lattice, (5) the LO phonons are taken to be the bulk phonons (3D) of GaAs, and (6) the first-order Born approximation for weak electron-LO-phonon interaction is used. In the linear regime the present balance equation approach is equivalent to the Kubo formula. The general trends in the linear magnetophonon resonances in the 2D EG in a GaAs- $\text{Al}_x\text{Ga}_{1-x}\text{As}$ heterostructure are similar to the 3D GaAs case; i.e., (1) the relative amplitude of the main peak is about 10% at $T=220$ K and (2) the amplitude of the magnetophonon resonance peaks as a function of temperature has a broad maximum around 200 K. A difference with the 3D case is the im-

portant effect of Landau-level broadening. Without broadening the magnetophonon resonance peaks are δ -function singularities in 2D, while in 3D only a logarithmic divergence is found at resonance. It appears from the present calculations that a Lorentzian form for the electron density of states gives slightly different results as compared to a Gaussian form with a flat background term. The latter form was recently suggested by experimental studies²⁴⁻²⁷ on the 2D density of states.

The energy relaxation rate of the 2D EG also shows magnetophonon resonances. Within an electron temperature model the amplitude of the magnetophonon resonances in the energy relaxation rate were found to be much larger than in the resistivity. Within this electron temperature model, the amplitude of the magnetophonon resonances in the resistivity increases with the electron temperature: (1) to above the 1% level for lattice temperature $T = 4.2$ K when $T_e > 40$ –50 K; this agrees with the observation of Ref. 16; and (2) the amplitude of the magnetophonon resonances increases much faster with T_e than with lattice temperature.

The warm-electron coefficient β_v , defined from the expansion of the momentum-balance equation to the first nonlinear order in the velocity, is a measure for the derivative of the transverse resistivity with respect to the electric field. β_v shows pronounced structure and increases strongly with decreasing temperature. For a Gaussian broadening without a flat background, β_v is negative near the linear magnetophonon resonance condition and positive far from resonance. This is again qualitatively similar to the 3D case. The quantitative behavior of β_v , even its sign, is extremely sensitive to the actual form of the 2D density of states. Other scattering mechanisms should also be included in the calculation of the linear resistivity in order to make quantitative predictions for realistic systems.

A numerical solution of the full velocity dependence

of the transverse resistivity shows (1) that the magnetophonon resonance maxima convert into minima when the average velocity of the electron $v > v_{LO}/10$ (similarly the minima convert into maxima at the same velocity), (2) a saturation region in the velocity for $T = 77$ K which is almost independent of the strength of the magnetic field, and (3) a monotonous decrease of the resistivity for very large velocities ("runaway"). Although in principle one should have to solve the coupled set of momentum- and energy-balance equations we believe that the present calculation of the nonlinear resistivity shows the correct general trends. The change of sign of the magnetophonon resonance extrema in the second derivative of $\rho_{xx}(B)$ was recently observed by Eaves *et al.*^{17,18} in an $n^+n^-n^+$ GaAs structure where the conduction is three dimensional. They analyzed the experimental results in terms of spatial Landau-level (LL) overlap due to the electric field. The conversion of maxima into minima was attributed to elastic inter-LL scattering and the contribution to ρ_{xx} of elastic electron acoustic-phonon scattering was estimated (they did not include the LO-phonon scattering). In the present model we find that a conversion of the magnetophonon resonance maxima into minima can also be induced by the interaction with LO phonons. A similar conclusion was reached in Ref. 7. Finally, we hope that these results will stimulate further experimental and theoretical investigations on linear and nonlinear transport in 2D EG in the presence of a magnetic field.

ACKNOWLEDGMENTS

This work was sponsored by I.I.K.W. (Interuniversitair Instituut voor Kernwetenschappen), Project No. 4.0002.83, Belgium. One of us (F.M.P.) would like to thank the National Fund for Scientific Research (N.F.W.O.), Belgium, for financial support.

*Also at University of Antwerp (Rijksuniversitair Centrum Antwerpen) and Eindhoven University of Technology, NL-5600 MB Eindhoven.

¹V. L. Gurevich and Yu. A. Firsov, *Zh. Eksp. Teor. Fiz.* **40**, 199 (1981) [*Sov. Phys.—JETP* **13**, 137 (1961)].

²R. J. Nicholas, *Prog. Quantum Electron.* **10**, 1 (1985).

³R. L. Peterson, in *Semiconductors and Semimetals*, edited by R. K. Willardson and A. C. Beer (Academic, New York, 1975), Vol. 10, Chap. 4.

⁴R. V. Parfenev, G. I. Kharus, I. M. Tsidilkovskii, and S. S. Shalyt, *Usp. Fiz. Nauk* **112**, 3 (1974) [*Sov. Phys.—Usp.* **17**, 1 (1974)].

⁵R. Lassnig and W. Zawadzki, *J. Phys. C* **16**, 5435 (1983).

⁶P. Vasilopoulos, *Phys. Rev. B* **33**, 8587 (1986).

⁷P. Vasilopoulos, M. Charbonneau, and C. M. Van Vliet, *Phys. Rev. B* **35**, 1334 (1987).

⁸D. C. Tsui, Th. Englert, A. Y. Cho, and A. C. Gossard, *Phys. Rev. Lett.* **44**, 341 (1980).

⁹G. Kido, N. Miura, H. Ohno, and H. Sakaki, *J. Phys. Soc. Jpn.* **51**, 2168 (1982).

¹⁰Th. Englert, D. C. Tsui, J. C. Portal, J. Beerens, and A. C. Gossard, *Solid State Commun.* **44**, 1301 (1982).

¹¹J. C. Portal, J. Cisowski, R. J. Nicholas, M. A. Brummell, M. Razeghi, and M. A. Poisson, *J. Phys. C* **16**, L573 (1983).

¹²M. A. Brummell, R. J. Nicholas, M. Razeghi, and M. A. Poisson, *Physica B + C* **117-118**, 753 (1983).

¹³R. J. Nicholas, L. C. Brunel, S. Huant, K. Karrai, J. C. Portal, M. A. Brummell, M. Razeghi, K. Y. Cheng, and A. Y. Cho, *Phys. Rev. Lett.* **55**, 883 (1985).

¹⁴M. A. Brummell, R. J. Nicholas, M. A. Hopkins, J. J. Harris, and C. T. Foxon, *Phys. Rev. Lett.* **58**, 77 (1987).

¹⁵M. Inoue, H. Hida, M. Inayama, Y. Inuishi, K. Nanbu, and S. Hiayamizu, *Physica B + C* **117&118B**, 720 (1983).

¹⁶H. Sakaki, K. Hirakawa, J. Yoshino, S. P. Svensson, Y. Sekiguchi, T. Hotta, and S. Nishii, *Surf. Sci.* **142**, 306 (1984).

¹⁷L. Eaves, P. S. S. Guimaraes, J. C. Portal, T. P. Pearsall, and G. Hill, *Phys. Rev. Lett.* **53**, 608 (1984).

¹⁸P. S. S. Guimaraes, L. Eaves, F. W. Sheard, J. C. Portal, and G. Hill, in *Proceedings of the Fourth International Conference on Hot Electrons in Semiconductors* [*Physica B + C* **134**, 47 (1985)].

¹⁹K. K. Thornber and R. P. Feynman, *Phys. Rev. B* **1**, 4099 (1970).

²⁰F. M. Peeters and J. T. Devreese, *Phys. Rev. B* **23**, 1936

- (1981).
- ²¹J. Shah, A. Pinczuk, A. C. Gossard, and W. Wiegmann, *Phys. Rev. Lett.* **54**, 2045 (1985).
- ²²J. Shah, in *The Physics of the Two-Dimensional Electron Gas*, edited by J. T. Devreese and F. M. Peeters (Plenum, New York, 1987).
- ²³T. Ando, B. Fowler, and F. Stern, *Rev. Mod. Phys.* **54**, 437 (1982).
- ²⁴E. Gornik, in *The Physics of the Two-Dimensional Electron Gas*, edited by J. T. Devreese and F. M. Peeters (Plenum, New York, 1987).
- ²⁵E. Gornik, R. Lassnig, G. Strasser, H. L. Störmer, A. C. Gossard, and W. Wiegmann, *Phys. Rev. Lett.* **54**, 1820 (1985).
- ²⁶J. P. Eisenstein, H. L. Störmer, V. Narayanamurti, A. Y. Cho, and A. C. Gossard, *Phys. Rev. Lett.* **55**, 875 (1985).
- ²⁷E. Stahl, D. Weiss, K. von Klitzing, and K. Ploog, *J. Phys. C* **18**, L783 (1985).
- ²⁸R. R. Gerhardts, *Z. Phys. B* **21**, 275 (1975).
- ²⁹E. Brezin, D. I. Gross, and C. Itzykson, *Nucl. Phys. B* **235**, 24 (1984).
- ³⁰R. R. Gerhardts and V. Gudmundsson, *Phys. Rev. B* **34**, 2999 (1986).
- ³¹V. Gudmundsson and R. R. Gerhardts, *Phys. Rev. B* **35**, 8005 (1987).
- ³²A. L. Fetter and J. D. Walecka, *Quantum Theory of Many-Particle Systems* (McGraw-Hill, New York, 1971).
- ³³W. Cai, X. L. Lei, and C. S. Ting, *Phys. Rev. B* **31**, 4070 (1985).
- ³⁴R. Kubo, S. J. Miyake, and N. Hatshitsume, in *Solid State Physics*, edited by F. Seitz and P. Turnbull (Academic, New York, 1965), Vol. 17.
- ³⁵F. M. Peeters and J. T. Devreese, *Phys. Rev. B* **25**, 7281 (1982).
- ³⁶F. M. Peeters and J. T. Devreese, *Phys. Rev. B* **31**, 3689 (1985).
- ³⁷T. Ando, *J. Phys. Soc. Jpn.* **38**, 989 (1975).
- ³⁸P. J. Price, *Ann. Phys. (N.Y.)* **133**, 217 (1981).
- ³⁹R. Lassnig and W. Zawadzki, *Surf. Sci.* **142**, 388 (1984).
- ⁴⁰*Physics of Group IV Elements and III-V Compounds*, Vol. 17a of *Landolt-Börnstein*, edited by O. Madelung, H. Schulz, and H. Weiss (Springer, Heidelberg, 1982).
- ⁴¹R. W. J. Hollering, T. T. J. M. Berendschot, H. J. A. Bluyssen, H. A. J. M. Reinen, and P. Wyder, in *Proceedings of the 18th International Conference on Physics of Semiconductors, Stockholm, 1986*, edited by O. Engström (World-Scientific, Singapore, 1987), p. 1323.
- ⁴²J. F. Ryan, R. A. Taylor, A. J. Turberfield, and J. M. Worlock, *Surf. Sci.* **170**, 511 (1986).
- ⁴³N. J. M. Horing, H. L. Cai, and X. L. Lei, *Phys. Rev. B* **35**, 6438 (1987).
- ⁴⁴C. Hamaguchi, T. Shirakawa, T. Yamashita, and J. Nakai, *Phys. Rev. Lett.* **28**, 1129 (1972).